

## Preparation and Characterization of TiO<sub>2</sub>-LaFeO<sub>3</sub> based Mixed Matrix Membrane for Oily Wastewater Treatment

R. Patrick<sup>a</sup>, F. Aziz<sup>a,b\*</sup>, N. Yahya<sup>a,b</sup>, N. A. Jamaludin<sup>a,b</sup>, N. M. Ismail<sup>c</sup>

<sup>a</sup>Faculty of Chemical and Energy Engineering, Universiti Teknologi Malaysia, 81310 UTM Johor Bahru, Johor, Malaysia

<sup>b</sup>Advanced Membrane Technology Research Centre (AMTEC), Universiti Teknologi Malaysia, 81310 UTM Johor Bahru, Johor, Malaysia

<sup>c</sup>Faculty of Engineering, Universiti Malaysia Sabah, Jalan UMS, 88400, Kota Kinabalu, Sabah, Malaysia.

### ABSTRACT

The aim of this study was to investigate the effects of catalyst loading in mixed matrix membrane. LaFeO<sub>3</sub> and TiO<sub>2</sub>-LaFeO<sub>3</sub> were synthesized by sol-gel glucose method. Fourier transform infrared spectroscopy (FTIR), scanning electron microscope (SEM), contact angle, membrane permeation testing unit and UV-Vis spectrophotometer techniques are used for characterization. FTIR showed the successful transformation of photocatalyst TiO<sub>2</sub>, LaFeO<sub>3</sub> and TiO<sub>2</sub>-LaFeO<sub>3</sub>. Due to increase in nanoparticles loading, the hydrophilicity of the membrane had improved thus increase the permeation flux. The cross-section morphology of membranes (PTL-1, PTL-3 and PTL-4) indicated that all the membranes were found to have asymmetric structure, consisting of dense top layer (air side), a porous sublayer (finger-like) and a small portion of sponge-like bottom surface layer (glass side). But as for the PTL-2, the cross sections of the membranes have a fully sponge-like structure. The formation of sponge-like structure was associated to the slow solidification process during the casting. The highest oily wastewater rejection was 76.26% with highest permeation flux and lower contact angle. This result showed that nanoparticles with membrane had improved the oily wastewater rejection. It proved that the fabricated nanoparticles with mixed matrix membrane exhibits a high flux, which is 2 to 3 orders of magnitude higher than commercial filtration membranes with an acceptable separation performance.

*Keywords:* Photocatalyst, oily wastewater, mixed matrix membrane, nanocomposites

### 1.0 INTRODUCTION

Water pollution due to organic compounds remains a serious environmental and public problem. The presence of micropollutants in the environment, the so-called emerging contaminants, has raised a great concern among the scientific community during the last few years [1]. Advanced treatment methods are improved to remove persistence and toxic matters [2]. Therefore, there is a need to develop technologies that can remove these pollutants from

wastewaters [1]. Oily waste water is one of the main causes of water pollution. It comes from oil field produced water, metal cleaning fluid and the waste emulsion in iron and steel works. With industrial development, there is increase in the amount of oil used, but various technical and management developments lag behind other reasons that are not perfect and make a lot of oil into the water, forming pollution [3]. The oil in the oil industry, oil refining, oil storage, transportation and petrochemical industries in the

\* Corresponding to: Farhana Aziz (email: [farhanaaziz@utm.my](mailto:farhanaaziz@utm.my))

production process generate lot of oily wastewater since we know that treating oily wastewater sources are very broad.

Membrane separation technology is the use of a special porous material manufactured for the interception role in the physical removal of a certain way of the trapped particle size of contaminants [3]. The advantages of membrane technology are that it works without addition of chemicals, with lower energy requirement, is easy to handle and has well-arranged process conduction [9]. These are characterized by their ability to remove suspended or colloidal particles by a sieving mechanism based on the size of the membrane pores [8].

A typical mixed-matrix membrane contains a dispersion of nanoparticles in bulk continuous polymer phase. With the incorporation of inorganic particles within the polymer matrix, the mixed-matrix membranes inherit some of the characteristics of inorganic particles, especially their superior separation performance [5]. Yuliwati and Ismail, studied a submerged system for oily wastewater treatment using mixed matrix membranes. The PVDF ultrafiltration membranes were prepared using pore-forming and hydrophilic additives and focused on the effect membrane morphology and transport properties [5].

Mixed matrix membranes have demonstrated better impact in oily wastewater treatment. Hydrophilic nature of the metal oxides and mechanical stiffness of the polymers combined influenced oily wastewater treatment. In addition, mixed matrix membranes were lagging in commercialization by their own defects. Symmetric dispersion of nanoparticles, uncontrol on pore size and leaching of nanoparticles in coagulation bath are major drawbacks in mixed matrix membrane [5].

Titanium oxide ( $\text{TiO}_2$ ) nanomaterial have been used widely for photocatalytic degradation of organic pollutants because it is effective, photo-stable, cheap, non-toxic and easy available [7]. Many researchers had done some approaches to modify the properties of  $\text{TiO}_2$  by combined it with other perovskites to form nanoparticles.

From previous research, finger like voids formation (from near the skin layer) in mixed matrix membranes containing  $\text{Co/TiO}_2$  can be attributed to hydrophilicity of nanoparticles which increase water diffusion (from non-solvent bath to dope) and exchange rate. However, by increasing the nanoparticles content to 1 wt.%, viscosity increase compensated solution hydrophilicity increase and results in low water diffusion rate is expectable [6]. Besides, when dispersed to PVDF membrane, a  $\text{TiO}_2$  nanoparticle not only improves the hydrophilicity of the membrane to enhance the flux but also kills the bacteria and mitigates the fouling problem of the PVDF membrane in the MBR system [5].

Lanthanum Orthoferrite ( $\text{LaFeO}_3$ ) is a better photocatalyst than  $\text{Fe}_2\text{O}_3$  due to its comparative electronic properties. such as electron-hole separation, mobility, photoexcited lifetimes and others is important for further development in ferrite-based photocatalyst [4].  $\text{LaFeO}_3/\text{TiO}_2$  composite nearly 90% of methyl orange (MO) gets decomposed after 180 min visible light radiation [13].  $\text{LaFeO}_3$  plays an important role in extending light absorption into the visible region and  $\text{TiO}_2$  can inhibit the recombination between photoinduced electron and hole pair [13]. It was found that the photocatalytic activity of the  $\text{LaFeO}_3/\text{TiO}_2$  composite gets enhanced due to the effect of  $\text{TiO}_2$ .

Many types of polymeric membrane

had been used such as polysulfone (Psf), polyethersulfone (PES), polyvinylidene fluoride (PVDF), polyether imide (PEI), polyacrylonitrile (PAN) and cellulose acetate (CA) for wastewater treatment [9].

Polymeric membranes have some advantages including high efficiency to remove particles, emulsified and dispersed oil; small size; low energy requirements; and inexpensive to that of ceramic-based membranes but it has disadvantages such as inability to separate volatile compounds and tendency to foul more quickly which results in flux decline and rejection deterioration for treating oily wastewater [9]. Polyetherimide (PEI) also been utilizing for treating oily wastewater. PEI is more convenient to become highly porous membrane because of the lower viscosity it possesses compared to PVDF.

The unique electronic, magnetic, and optical properties of nanoparticles improved the capabilities of the polymer in a certain extent because of their small sizes, large ratio surface areas, and strong activities. The presence of finely dispersed inorganic particles in the polymer matrix has proven very useful in the improvement of membrane performance.<sup>5</sup> Blending approach has been extensively utilized for polymeric membrane fabrication due to its facile preparation procedure, versatility to incorporate desirable properties on the membrane, and its profound ability to simultaneously modify the membrane properties during the phase inversion process [9].

In this study, TiO<sub>2</sub>-LaFeO<sub>3</sub> nanocomposites were incorporated into PEI polymer to produce mixed matrix membranes (MMM) for oily wastewater treatment. The fabricated MMM were then characterized using Fourier transform infrared spectroscopy (FTIR), scanning

electron microscope (SEM), contact angle, membrane permeation testing unit and UV-Vis spectrophotometer. The effect photocatalyst loading in photocatalytic membrane were also investigated. The PEI membranes have been fabricated with TiO<sub>2</sub>-LaFeO<sub>3</sub> in various concentrations to modify membrane properties and filtration performance. FTIR spectrometer is used for the functional group identifications of perovskite. The morphological properties of the MMM are studied using scanning electron microscope (SEM). The membrane hydrophilicity is determined by measuring the contact angle. Performance test had been conducted using membrane permeation testing unit. For determination of oily wastewater rejection using UV-Vis spectrophotometer.

## 2.0 METHODS

### 2.1 Materials Preparation

The solvent N, N-dimethylacetamide (DMAc, Aldrich Chemical) (Synthesis Grade, Merck, N 99%) was used as polymer solvent without further purification. Iron (III) nitrate nanohydrate [Fe(NO<sub>3</sub>)<sub>3</sub>•9H<sub>2</sub>O], lanthanum (III) Nitrate [La(NO<sub>3</sub>)<sub>3</sub>], glucose powders, Titanium Oxide (TiO<sub>2</sub>) powder from Aldrich Chemical and Polyetherimide (PEI). Synthetic oil was used for oily wastewater treatment.

### 2.2 Synthesis of LaFeO<sub>3</sub> by Sol-gel Method

Lanthanum (III) nitrate [La(NO<sub>3</sub>)<sub>3</sub>], iron (III) nitrate nanohydrate [Fe(NO<sub>3</sub>)<sub>3</sub>•9H<sub>2</sub>O] (98.5%), glucose (99.945%) and 65-68% nitric acid were employed as the starting ingredients. A 80% glucose solution

was made by adding glucose powders to deionized water. Then,  $\text{La}(\text{NO}_3)_3$  and glucose solution were mixed by stirring at  $60^\circ\text{C}$ . Finally,  $\text{Fe}(\text{NO}_3)_3 \cdot 9\text{H}_2\text{O}$  was added to the solution. During the process, the mole ratios of glucose to metal ions (glucose/M) were 3:5. With continuous heating at  $70^\circ\text{C}$  under constant stirring to evaporate superfluous water, the volume of the solution decreased and the solution viscosity increased continuously.

A gel was formed with evolution of  $\text{NO}_x$  gas resulting from decomposition of nitrate ions. Throughout the process, no signs of precipitation are observed. Then, the sample was removed from the hot plate and heated in an oven at  $250^\circ\text{C}$  for 2 hours. The resulting product was slightly ground into fine powder and  $\text{LaFeO}_3$  precursor was obtained. The precursor was calcined at  $600^\circ\text{C}$  for 2 hours in air to obtain  $\text{LaFeO}_3$  powder.

### 2.3 Synthesis of $\text{TiO}_2$ - $\text{LaFeO}_3$ by Sol-gel Method

The preparation of  $\text{LaFeO}_3$ - $\text{TiO}_2$  (2:1 M ratio) was as follows: Beaker A: Weighed 0.60 g of  $\text{TiO}_2$  powder. Beaker B: 1.20 g of  $\text{LaFeO}_3$  was dissolved in distilled water and stirred continuously for 2 hours. After that the solution was ultrasonicated to get the uniform distribution. Finally,  $\text{TiO}_2$  powder in beaker A was added slowly into solution in the beaker B under vigorous stirring. After stirring for 4 hours at room temperature, let the solution rest for 1 hour. Then, filtrated the distilled water using filter paper. The remaining solution that contain product was dried in the furnace at  $60^\circ\text{C}$  for overnight. The resultant product will be further calcinated at  $600^\circ\text{C}$  for 3 hours to obtain  $\text{TiO}_2$ - $\text{LaFeO}_3$  powder.

### 2.4 Preparation of Synthetic Oily Wastewater

The synthetic oil wastewater was prepared by mixing tap water with synthetic oil (10 wt%). The solution was then stirred for 30 min with an agitation speed of 500 rpm at room temperature.

### 2.5 Preparation of Dopes

Table 1 summarises the dope composition of mixed matrix membrane preparation. An amount of pre-dried (24 hours oven dried at  $60^\circ\text{C}$ ) PEI pellets were weighed and poured into pre-weighed DMAc solvent. The mixture was stirred to ensure thorough wetting of polymer pellet.  $\text{TiO}_2$ - $\text{LaFeO}_3$  was dissolved in pre-weighed DMAc solvent and ultrasonicated for 30 minutes to get the uniform distribution. Then, the solution was added to the polymer dope mixtures which were continuously stirred for 48 hours at 500 rpm until a homogenous solution was formed. The polymer solution was kept in a glass bottle and air bubbles form in the dope was removed using ultrasonic bath for several hours. The fully dissolved polymer solution was allowed stand and degassed for 1 hour at room temperature for casting.

**Table 1** Dope composition for mixed matrix flat sheet preparation

Sample	PEI (wt%)	$\text{TiO}_2$ - $\text{LaFeO}_3$ (wt%)	DMAc (wt%)
PTL-1	16	0	84.00
PTL-2	16	0.13	83.87
PTL-3	16	0.27	83.73
PTL-4	16	0.40	83.60

## 2.6 Fabrication of Flat-sheet Membrane by Phase Inversion Immersion Precipitation (Casting)

A certain amount of PEI/ TiO<sub>2</sub>-LaFeO<sub>3</sub> solution was poured over a glass plate and was gently lathered by a casting roll glass. Then, the lathered film solution was immediately immersed into a coagulation bath (tap water) for 1 hour. After completing coagulation, the membrane was transferred and immersed into another coagulation bath (tap water) for 24 hours to remove the residual solvents, and afterwards, it was rinsed with tap water, followed by drying in the air at room temperature until a dry flat sheet membrane was obtained.

## 2.7 Characterization

### 2.7.1 Scanning Electron Microscope (SEM)

The morphology of the membrane was observed by scanning electron microscope (SEM) (Hitachi TM 3000 Tabletop Microscope). The SEM micrographs are taken at certain magnifications. It will produce photographs at the analytical working distance of 10000 m.

### 2.7.2 Contact Angle (CA)

The membrane hydrophilicity was determined by measuring the contact angle. The membrane contact angle (CA) was measured by the sessile drop method using an optical sub-system (SCA 20) integrated with image-processing software. Sample membranes were placed on a platform, and droplets of 0.5 mL are dropped carefully on the membrane surface. A real-time camera captured the image of the droplet, and the CA was estimated by a computer. At least 5

measurements were taken for each membrane sample.

### 2.7.3 Membrane Permeation Testing Unit

The pure water flux and rejection were measured using the membrane permeation testing unit. The flat sheet membrane was cut to a circular disk before it was installed in the membrane cell. The permeation flux was conducted with a pressure of 2 bar at the beginning, testing until the water flowed under steady conditions. Then, 1 bar of pressure was applied to determine the value of pure water flux and rejection. The value of pure water flux was recorded every 10 min. The rejection measurement was carried out using synthetic oily wastewater solution at a pressure of 1 bar. The pure water flux was measured using equation (1) at pressure of 1 bar. Where J is permeation flux (L/m<sup>2</sup>hr), V is the permeate volume (L), A is the membrane area (m<sup>2</sup>) and is filtration time (hour).

$$J = \frac{V}{A \times \Delta t} \quad (1)$$

### 2.7.4 UV-vis Spectrophotometer

The UV-vis absorption spectrum was carried out using UV-spectrophotometer (HACH Model DR5000) at  $\lambda = 545$  nm. The rejection of oily wastewater degraded was determined using Equation (2). Where C<sub>0</sub> is the concentration of oily wastewater feed and C<sub>t</sub> is the concentration of oily wastewater permeates. The higher rejection value shows the most effective membrane.

$$\text{Rejection (\%)} = \frac{C_0 - C_t}{C_0} \times 100\% \quad (2)$$

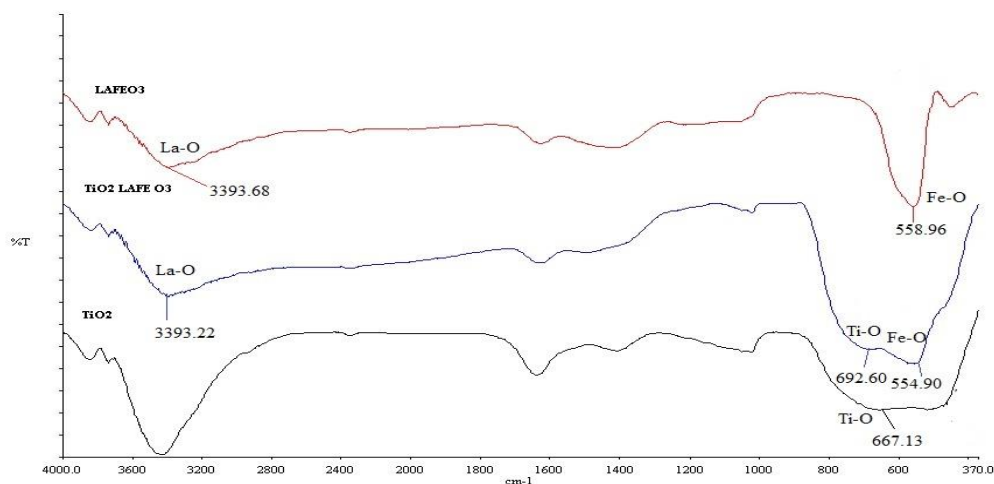


**Figure 1** FTIR spectra of  $\text{TiO}_2$ ,  $\text{LaFeO}_3$  and  $\text{TiO}_2$ - $\text{LaFeO}_3$  sample

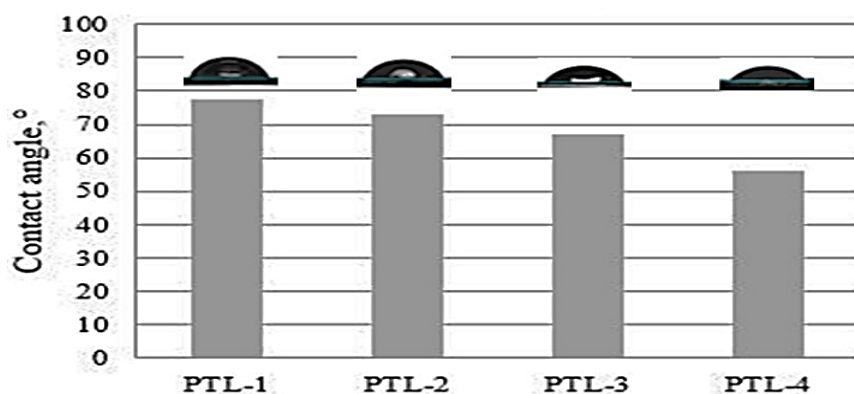


**Figure 2** Contact angle for PEI/ $\text{TiO}_2$ - $\text{LaFeO}_3$  samples

### 2.7.5 Fourier Transform Infrared Spectroscopy (FTIR)

Spectrum one FTIR spectrometer was used for the functional group identifications of perovskite. The FTIR measurements had been performed in the potassium bromide mode (KBr) using the model 6300 FTIR spectrometer.

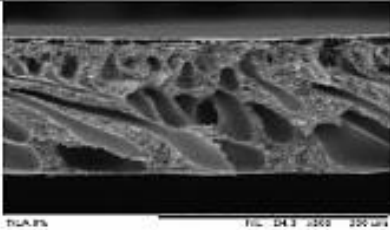
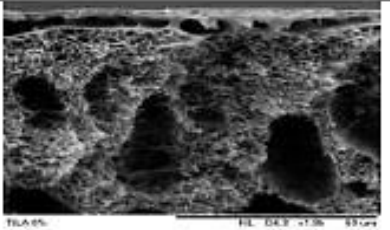
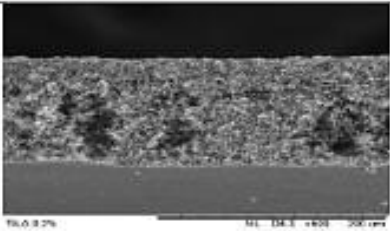
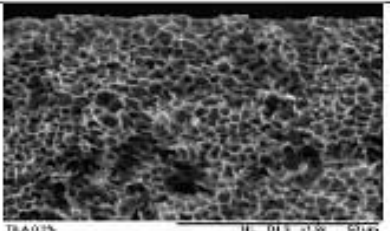
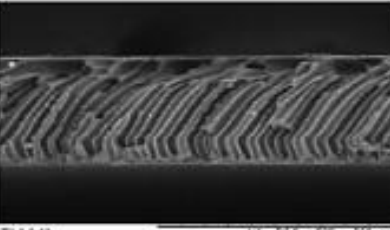
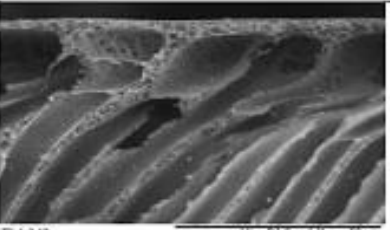
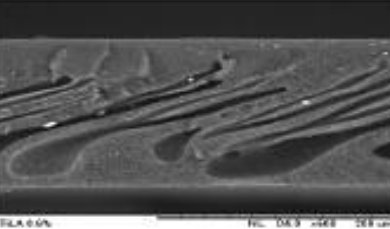

## 3.0 RESULTS AND DISCUSSION

### 3.1 Fourier Transform Infrared Spectroscopy (FTIR)

Based on Figure 1, for  $\text{LaFeO}_3$  sample, the sharp absorption band at  $558.96 \text{ cm}^{-1}$  attributed to B-O (Fe-O)

stretching vibration, being characteristics of the octahedral  $\text{BO}_6$  groups in the perovskite (ABO) compound, which was commonly observed in the region  $500\text{-}700 \text{ cm}^{-1}$  (Feng *et al.* 2011, Abazari *et al.* 2013). The absorption band at  $3393.68 \text{ cm}^{-1}$  had attributed to La-O stretching vibration. For pure  $\text{TiO}_2$ , the absorption band was  $667.13 \text{ cm}^{-1}$  corresponded to Ti-O stretching vibration and this vibration confirmed the formation of rutile phase of  $\text{TiO}_2$  nanoparticles. But as for the  $\text{TiO}_2$ - $\text{LaFeO}_3$  nanocomposite, it exhibited all the three-stretching absorption bands La-O, Fe-O and Ti-O which confirmed the formation of  $\text{TiO}_2$ - $\text{LaFeO}_3$  nanocomposites.

**Table 2** Cross Section and top layer image of membrane

Sample	Cross section at 500× magnification	Top layer at 1.8k× magnification
PTL-1		
PTL-2		
PTL-3		
PTL-4		

### 3.2 Contact Angle

Based on Figure 2, it was clear that PEI membrane without photocatalyst (PTL-1) has a higher contact angle of value 77.33° and lowest contact angle of value 56.17° as there was increase in amount of photocatalyst loading. With the addition of TiO<sub>2</sub>-LaFeO<sub>3</sub>, hydrophilicity is enhanced. It is also clear that TiO<sub>2</sub> has good affinity with La-O and Fe-O groups and thus mutual functionalities (hydrophilicity) aid in improving the water permeability since the contact angle for PEI/LaFeO<sub>3</sub> was 69.73°.

### 3.3 Scanning Electron Microscope (SEM)

The morphology of the membranes was studied by SEM to represent the cross-sectional and top layer at a certain magnification. Table 2 shows the SEM micrographs of the PEI membranes prepared using different concentrations of TiO<sub>2</sub>-LaFeO<sub>3</sub>. The improvement of membrane morphology occurs with a small amount addition of nanoparticles. However, with further increasing TiO<sub>2</sub>-LaFeO<sub>3</sub> concentration, it was observed that the cross section of membrane had



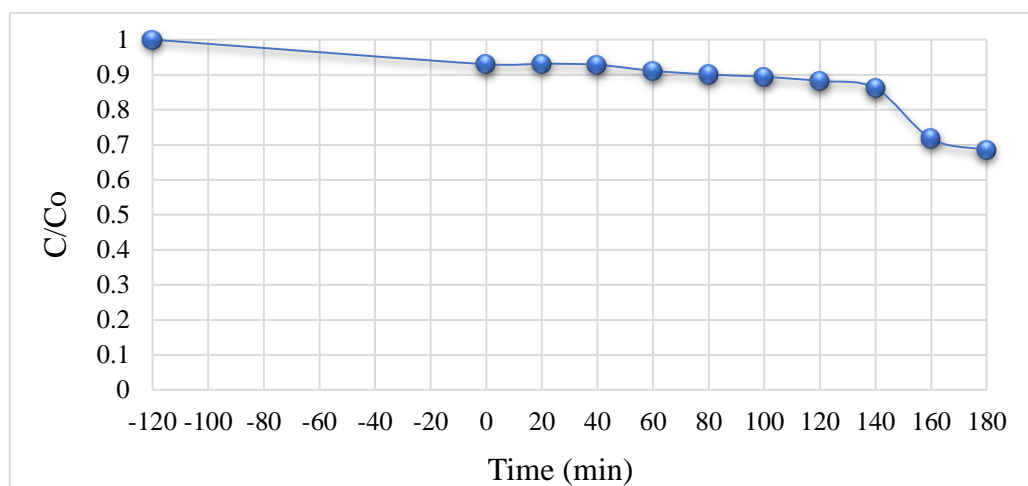


**Figure 1** UV-Vis time dependent absorption spectra during photocatalytic reaction of MB for  $\text{TiO}_2\text{-LaFeO}_3$  nanocomposites

been changed significantly. It indicated that the hydrophilicity of nanoparticles was directly correlated with lower contact angle and might be responsible for the higher liquid uptake. This may be attributed to the increase of wettability on the membrane surface. The cross-section morphology of membranes (PTL-1, PTL-3 and PTL-4) indicated that all the membranes were found to have asymmetric structure, consisting of dense top layer (air side), a porous sublayer (finger-like) and a small portion of sponge-like bottom surface layer (glass side). But as for the PTL-2, the cross sections of the membranes have a fully sponge-like structure. The formation of sponge-like layer was associated to the slow solidification process during the casting. PTL-4 had shown the agglomeration of nanoparticles on top layer and bottom layer of membrane. This agglomeration of nanoparticles caused the blockage of pores and thus decreased the permeation flux and oily wastewater rejection.

### 3.4 Photocatalytic Study

The degradation of methyl blue (MB) with  $\text{TiO}_2\text{-LaFeO}_3$  samples was kept stirred in the dark condition for 2 hours

so that the adsorption-desorption equilibrium was reached. After 2 hours, as the irradiation time was extended from 0 to 180 min under visible light, the intensity of the absorbance starts decreases from 0.585 a.u to 0.401 a.u. Hence, the results as shown in Figure 3 indicated that the absorbance was reduced as the radiation time increases. After 180 min, the absorbance was decrease to 0.401 a.u and the intense blue colour of the starting MB solution faded. For  $\text{TiO}_2\text{-LaFeO}_3$  nanoparticles, the photolysis of methyl blue was slow and about 36.45% of MB was decomposed after 180 min visible light radiation. This might due to effect of temperature since temperature was not control variable. Besides, the halogen lamp (visible light) became very hot as the time taken was increase to 180 minutes. The lowering in temperature favours the adsorption of the final reaction product, whose desorption tends to inhibit the reaction. On the contrary, when temperature tends to the boiling point of water, the exothermic adsorption of reactant becomes disfavoured and tends to limit the reaction (Mehrotra *et al.*, 2005).



### 3.5 Pure Water Flux and Oily Wastewater Rejection

Owing to the hydrophilicity effect of TiO<sub>2</sub>-LaFeO<sub>3</sub> catalyst embedded within membrane matrix, the permeate flux was reported to increase with increasing TiO<sub>2</sub>-LaFeO<sub>3</sub> loading from 0 to 0.4 wt% as shown in Figure 4. Similar results have also been reported by (Vernardou *et al.*, 2009), where they found that membrane hydrophilicity was remarkably increased (i.e. lower water contact angle) with increasing TiO<sub>2</sub> loading. Due to increase in nanoparticles loading, the hydrophilicity of the membrane had increase thus the permeation flux also increase. For oily wastewater, the permeation flux also increased but the oily wastewater permeation flux was lowered than

water permeation flux due to the formation of cake on the surface of the membrane as time passed. From the Table 3, the higher rejection of oily wastewater was 76.26%. From previous study, the hydrophilic TiO<sub>2</sub> particles, which contained hydroxyl groups and adsorbed on the membrane surface, were responsible for the increased hydrophilicity. Besides, the increased membrane hydrophilicity and membrane pore size with lower TiO<sub>2</sub> concentration (<1.95 wt.%) could attract water molecules inside the composite membrane; facilitated their penetration through the membrane, enhancing the flux and rejection (E. Yuliwati *et al.*, 2011). Based on the results obtained, it can be said that the membrane separation performance with 0.4wt.% TiO<sub>2</sub>-LaFeO<sub>3</sub> was therefore selected as the best catalyst

**Table 3** Average permeation flux and oily wastewater rejection for PEI/TiO<sub>2</sub>-LaFeO<sub>3</sub>

Sample	Average Permeation flux water, J (L/m <sup>2</sup> h)	Average Permeation flux oily wastewater, J (L/m <sup>2</sup> h)	Oily wastewater rejection, %
PTL-1	364.64	321.32	47.96
PTL-2	801.02	759.97	54.39
PTL-3	962.87	833.99	68.42
PTL-4	1508.03	1155.3	76.26

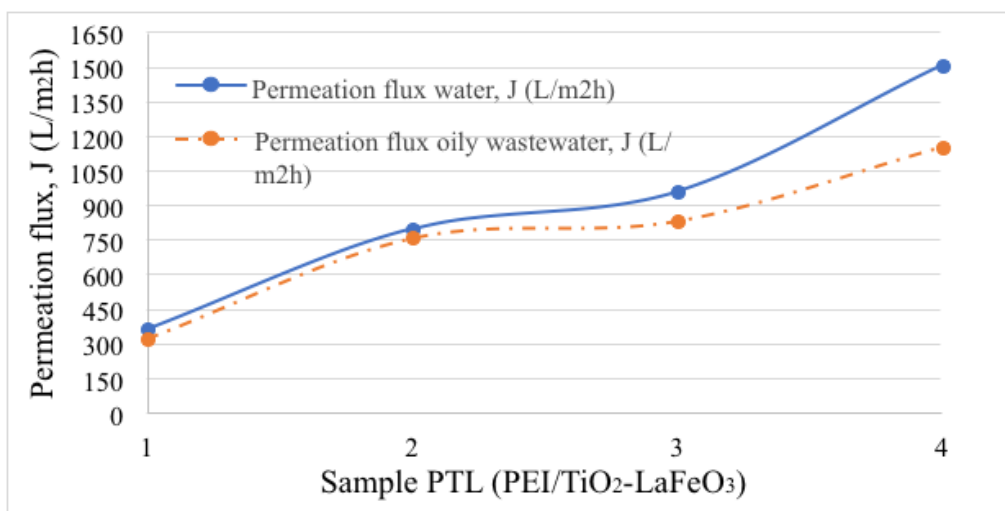


**Figure 2** Average permeation flux of water and average permeation flux of oily wastewater for PEI/TiO<sub>2</sub>-LaFeO<sub>3</sub>

loading. This result showed that nanoparticles with membrane had improved the oily wastewater rejection. These results proved that the fabricated nanoparticles with mixed matrix membrane exhibits a high flux, which is 2 to 3 orders of magnitude higher than commercial filtration membranes with an acceptable separation performance (Matos *et al.*, 2016).

#### 4.0 CONCLUSION

In conclusion, the photocatalyst that used was TiO<sub>2</sub>-LaFeO<sub>3</sub> and polymeric membrane was PEI for synthetic oily wastewater treatment. PEI flat sheet membranes were fabricated by casting. The rejection result from PEI/ TiO<sub>2</sub>-LaFeO<sub>3</sub> for synthetic oily wastewater treatment was 76.26% with highest water permeation flux and lower contact angle. The hydrophilicity of nanoparticles was directly correlated with lower contact angle and thus increase in permeation flux. Some modification might need to be done to further increase the hydrophilicity of the membrane. Besides, the equally dispersion of nanoparticles in membrane will help to improve the oily rejection and permeation flux.

#### ACKNOWLEDGEMENT

The authors acknowledge the financial support by the Ministry of Higher Education (MOHE) Malaysia under Grant (HiCOE) No. R.J090301.7846.4J189, R.J090301.7846.4J190 and Universiti Teknologi Malaysia (UTM).

#### REFERENCES

- [1] S. Khaoulani, H. Chaker, C. Cadet, C. Bychkov, L. Eugene and A. Bengueddach. 2015. Wastewater Treatment by Cyclodextrin Polymers and Noble Metal/mesoporous TiO<sub>2</sub> Photocatalysts. *Comptes Rendus Chimie*. 18(1): 23–31.
- [2] R. Ruth, M. Erol, F. Bakal, G. Oner and E. Çelik. 2015. Surface & Coatings Technology Photocatalytic Degradation of Cyanide in Wastewater Using New Generated Nano-Thin Film Photocatalyst. *Surface and Coating Technology*. 271: 207–216.
- [3] L. Yu, M. Han and F. He. 2013. A Review of Treating Oily Wastewater. *Arabian Journal of Chemistry*. <http://dx.doi.org/10.1016/j.arabjc.2013.07.020>. In Press.
- [4] P. Kanhere and Z. Chen. 2014. A Review on Visible Light Active Perovskite-based Photocatalysts. *Molecules*. 19(12): 19995-20022.
- [5] M. Padaki, R. Surya Murali, M. S. Abdullah, N. Misdan, A. Moslehyani, M. A. Kassim, N. Hilal and A. F. Ismail. 2015. Membrane Technology Enhancement in Oil-Water Separation. A Review. *Desalination*. 357: 197–207.
- [6] S. Narjes, A. Kamran and M. Ali. 2017. Photocatalytic Degradation of 2,4-Dichlorophenol by Co-Doped TiO<sub>2</sub> (Co/TiO<sub>2</sub>) Nanoparticles and Co/TiO<sub>2</sub> Containing Mixed Matrix Membranes. *Journal of Water Process Engineering*. 17: 124–34.
- [7] H. Zangeneh, A. Zinatizadeh, A. L. Habibi, M. Akia and M. Hasnain Isa. 2015. Photocatalytic

- Oxidation of Organic Dyes and Pollutants in Wastewater Using Different Modified Titanium Dioxides: A Comparative Review. *Journal of Industrial and Engineering Chemistry*. 26: 1-36.
- [8] R. Dhinesh Kumar, R. Thangappan and R. Jayavel. 2016. Synthesis and Characterization of LaFeO<sub>3</sub>/TiO<sub>2</sub> Nanocomposites for Visible Light Photocatalytic Activity. *Journal of Physics and Chemistry of Solids*. 101: 25-33.
- [9] E. Yuliwati and A. F. Ismail. 2011. Effect of Additives Concentration on the Surface Properties and Performance of PVDF Ultrafiltration Membranes for Refinery Produced Wastewater Treatment. *Desalination*. 273(1): 226-234.
- [10] H. Shen, T. Xue, Y. Wang, G. Cao, Y. Lu and G. Fang. 2016. Photocatalytic Property of Perovskite LaFeO<sub>3</sub> Synthesized by Sol-Gel Process and Vacuum Microwave Calcination. *Materials Research Bulletin*. 84: 15-24.
- [11] J. Feng, T. Liu, Y. Xu, J. Zhao, H. Yanyan and J. Ceram. 2011. Synthesis of Nanocrystalline LaFeO<sub>3</sub> Powders via Glucose Sol-Gel Route. *Materials Chemistry and Physics*. 12(3): 1047-1050.
- [12] V. K. Gupta and I. Ali. 2013. Chapter 5: Water Treatment by Membrane Filtration Techniques. *Environmental Water*. 135-154.
- [13] M. Matos, G. Gutiérrez, A. Lobo, J. Coca, C. Pazos and J. M. Benito. 2016. Surfactant Effect on the Ultrafiltration of Oil-in Water Emulsions Using Ceramic Membranes. *Journal of Membrane Science*. 520: 749-59.
- [14] D. Vernardou, G. Kalogerakis, E. Stratakis, G. Kenanakis E. Koudoumas and N. Katsarakis. 2009. Photoinduced Hydrophilic and Photocatalytic Response of Hydrothermally Grown TiO<sub>2</sub> nanostructured Thin Films. *Solid State science*. 11(8): 1499-1502.
- [15] R. Abazari and S. Sasnati. 2013. Perovskite LaFeO<sub>3</sub> Nanoparticles Synthesized by the Reverse Microemulsion Nanoreactors in the Presence of Aerosol-OT: Morphology, Crystal Structure and their Optical Properties. *Super Lattices and Microstructures*. 64: 148-157.
- [16] K. Mehrotra, G. S. Yablonsky, and A. K. Ray. 2005. Macro Kinetic Studies for Photocatalytic Degradation of Benzoic Acid in Immobilized Systems. *Chemosphere*. 60: 1427-1436.